PROCEEDINGS, 41st Workshop on Geothermal Reservoir Engineering
Stanford University, Stanford, California, February 22-24, 2016
SGP-TR-209

The Effect of Bottom Boundary Conditions on Predictions of Steam Production from Geothermal Reservoir Models

John O'Sullivan and Mike O'Sullivan

Department of Engineering Science, University of Auckland, Private Bag 92019 Auckland, New Zealand

jp.osullivan@auckland.ac.nz

Keywords: Geothermal reservoir modelling, boundary conditions, TOUGH2

ABSTRACT

A very large numerical model of a synthetic geothermal system has been created using the University of Auckland's improved air/water supercritical AUTOUGH2 code. The model extends from the surface to the brittle/ductile transition region at depth of 8 km and encompasses the system's entire geothermal plume. At the bottom boundary a heat anomaly is applied which creates a hot, liquid-dominated system similar to those found in New Zealand. A production scenario equivalent to 120MW was then run using the model and the results treated as the "true" history for the system.

Two smaller models were then created using the standard version of AUTOUGH2 with bottom boundaries above the supercritical region. Each model applied a different, common reservoir modelling approach at the bottom boundary. In both approaches a distributed constant mass flow is applied at the bottom boundary to represent the hot inflow from the deeper plume. However, for heat input the approaches differ. The first approach applied heat uniformly to the bottom boundary representing the background heat flux. The second approach applies a constant temperature ("hot-plate") boundary condition using inactive blocks at the base of the model. Both models accurately reproduced the natural state temperatures of the hypothetical system. However, for the production scenario both approaches underpredicted the total steam production with the hot-plate approach having a slightly larger error. The underprediction could be reduced when using either approach by calibrating the model parameters away from their "true" values.

1. INTRODUCTION

Reservoir models are important tools used for understanding and managing geothermal resources (Dipippo, 2016). A model's usefulness is defined by its ability to provide accurate predictions of the behaviour of a geothermal system. To develop reservoir models capable of providing accurate predictions, as many of the important characteristics of the system are included as possible (O'Sullivan *et al*., 2001). However, it is impossible to represent all of the important characteristics in a numerical model and simplifying assumptions must be made. In some cases this is because properties of the system are unknown and cannot be measured. In others it is a result of technical or computational limitations.

TOUGH2 (Pruess *et al*., 1999) is the industry standard tool for carrying out numerical simulations of geothermal reservoirs and the most commonly used versions of the software limit fluid conditions to below the critical temperature for water (~374° C). This technical limitation means that most reservoir models do not include the entire geothermal plume. Hence, the effect of deeper parts of the system can be included only as boundary conditions applied at the bottom of the model. There are several possible options but the two most commonly used are the background heat flux approach (Clearwater *et al*., 2011; O'Sullivan *et al*., 2016; Ratouis *et al*., 2016) and the "hot-plate" approach (Burnell and Kissling, 2005; Bjornsson and Arnaldsson, 2015; Gunnarsson and Aradóttir, 2015; Hernandez *et al*., 2015). In both approaches mass is injected into the bottom of the model to represent the deep upflow from the geothermal plume. However, they differ in their representation of the conductive heat flow from depth, with the background heat flux approach applying a fixed heat flux and the "hot-plate" approach applying a fixed temperature distribution.

Recently supercritical versions of the TOUGH2 simulator have been developed (Croucher and O'Sullivan, 2008; Magnusdottir and Finsterle, 2015) and the University of Auckland's improved air/water supercritical AUTOUGH2 code (O'Sullivan *et al*., 2015) can now be used to simulate the entire geothermal plume from the surface to the brittle/ductile transition region. By developing a large model of a hypothetical geothermal system and using the supercritical AUTOUGH2 simulator to generate detailed data describing the structure of the system, it is now possible to quantitatively assess the impact of developing smaller working models which use each of the bottom boundary condition approaches described above.

In the following section detailed descriptions are given of the hypothetical geothermal system and the large supercritical model that has been created to simulate its behaviour. The details of the two smaller working models are then presented and comparisons are made with the natural state predictions generated by each of them. The production history scenario that was developed and simulated using the supercritical model is then presented followed by comparisons with each of the working models and a discussion of the results.

The PyTOUGH library (Wellmann *et al*., 2012) was used extensively throughout this project to create models, control simulations and visualize results.

2. DESCRIPTION OF THE HYPOTHETICAL GEOTHERMAL SYSTEM

The hypothetical system was designed to have characteristics similar to those found in real hot, liquid-dominated geothermal systems hosted within volcanic settings (Grant, 2013). It consists of a reservoir approximately 8 km x 8 km beneath an area of raised topography with elevations ranging from 1000 mRL down to 500 mRL. The bottom of the conductive clay cap that has formed above the system can be found at 200 mRL and the reservoir extends down to a low permeability basement formation at -2000 mRL. A deeper basement formation extends from -3600 mRL down to the brittle/ductile transition region at a depth of 8 km.

a)

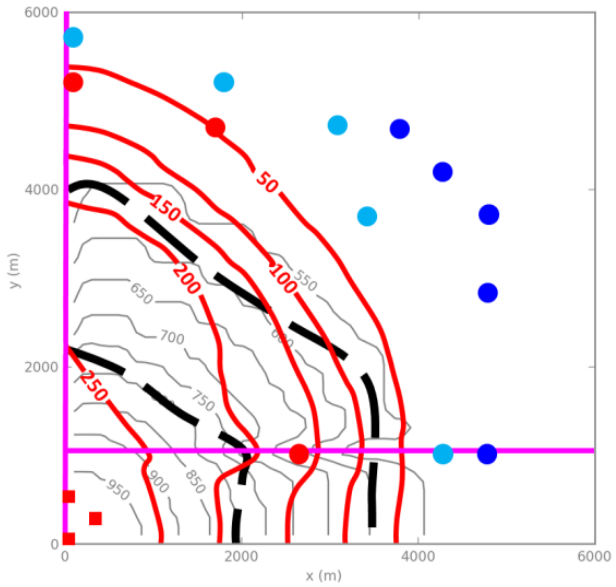

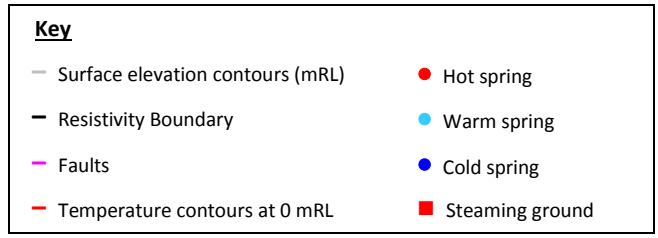

b)

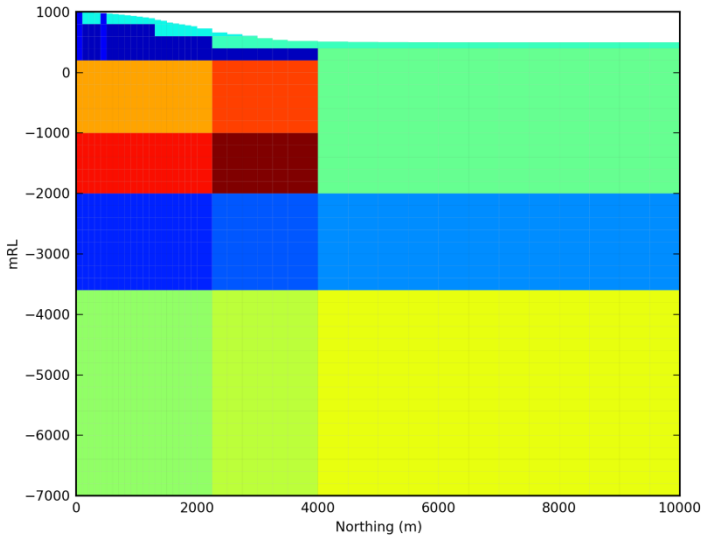

c)

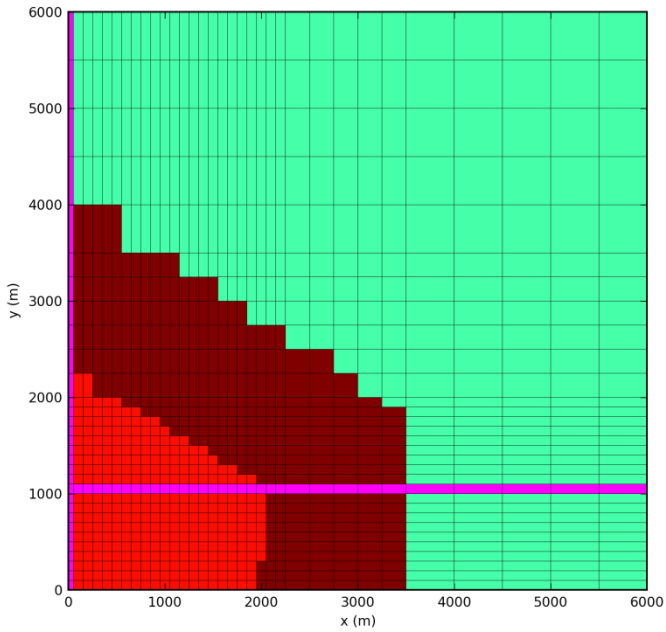

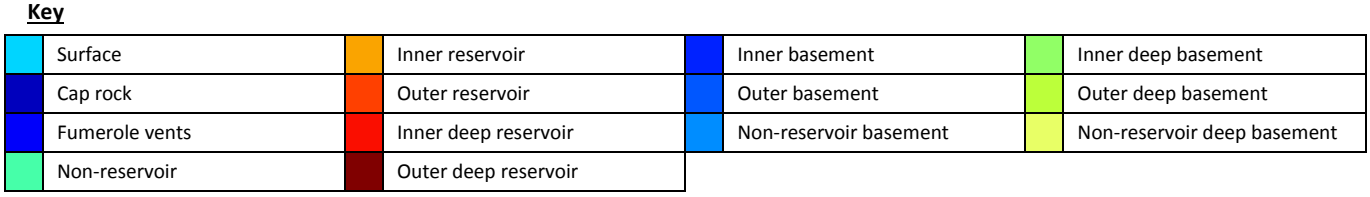

Figure 1: Plan view of the conceptual model (a). Cross section of system geology along line x = 0 m (b). System geology at 0 mRL with faulted rock types shown in magenta (c).

The system, shown in Figure 1, was made to be symmetric in both horizontal directions which reduced the computational cost of generating synthetic field data by a factor of four. While this simplification is acceptable in the context of boundary condition studies, it not only had implications for the shape of the reservoir and topography but also for the layout of the faults. Three vertical faults were created; one North-South fault passing through the center of the system and two East-West faults offset 1 km from the center.

The synthetic field data were generated by creating a high resolution model of the system with realistic parameters and then running simulations using the University of Auckland's improved air/water supercritical AUTOUGH2 code (O'Sullivan *et al*., 2015). The model covers a large area and has closed lateral boundaries thus simulating the entire convective plume and its recharge. At the top surface a dry air atmosphere was prescribed with meteoric recharge included equivalent to 1000 mm/yr of rainfall at 15° C with an infiltration rate of 8%. At the bottom of the model a background heat flux of 80 mW/m^2 was applied uniformly as well as a large, smooth, circular Gaussian heat anomaly located underneath center of the system. Figure 2 shows the distribution of the additional heat input which equates to 23 MW for the model or 92 MW for the entire system. The bottom boundary was closed to mass flow for this study though a small amount of magmatic water could easily be injected into future models.

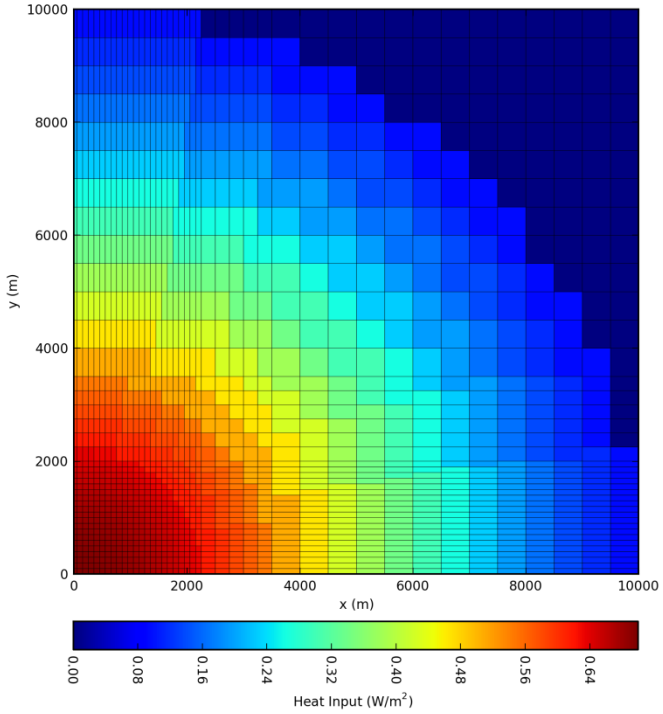

Figure 2: Heat anomaly at the bottom boundary of the synthetic model.

Along with the permeability structure Figure 1c shows the model grid is made up of 100 m x 100 m columns in the central region with columns of up to 500m x 500m at its edge. In the vertical direction a constant layer height of 200m was selected with incomplete layers used to represent the topography as shown in Figure 1b. The resulting model comprised a total of approximately 63000 blocks.

The set of parameters used for each of the different formations that resulted in the hot, liquid-dominated reservoir conditions are presented in Table 1. The permeabilities given for the faulted blocks in the formations refers to the maximum permeability which was applied either along the strike of the fault or vertically. In the present work none of the faults reduced or enhanced the permeability of the formation across their strike. Typical values of 2500 kg/m3, 2.5 W/m° C and 1000 J/kg° C were applied uniformly for the rock grain density, the formation heat conductivity and the rock grain specific heat. Linear relative permeability curves were selected with a residual water saturation of 0.5.

Table 1: Rock properties for main formations in the synthetic model

Rock type	Permeabilities (mD)			Porosity	
	x-y	z	Fault	Intact	Fault
Cap rock	0.5	0.2	-	0.1	-
Inner Reservoir	8	20	50	0.1	0.3
Outer Reservoir	2.5	10	20	0.1	0.3
Non-reservoir	1	0.5	5	0.1	0.15
Inner deep Reservoir	2	10	10	0.1	0.3
Outer deep Reservoir	1	5	10	0.1	0.3
Inner basement	0.7	2	2.5	0.05	0.2
Outer basement	0.7	1	1.5	0.05	0.2
Non-reservoir basement	0.7	0.35	1	0.05	0.2
Inner deep basement	0.5	2	2.5	0.02	0.1
Outer deep basement	0.5	0.5	1	0.02	0.1
Non-reservoir deep basement	0.4	0.2	0.5	0.02	0.1

2.1 Natural State Results

A large convective plume developed in the system which can be seen in the temperature cross section plotted in Figure 3a. It has a wide upflow zone occupying much of the inner reservoir with reservoir temperatures ranging from 250-300° C. The figure also shows that the deep upflow is structurally controlled with the faults acting as pathways for the rising hot fluid. At higher elevations the faults allow the plume to spread, elongating along the N-S axis. Temperature contours at 0 mRL are shown in Figure 1a as well as the locations of significant mass flows from surface blocks. These flows range from cold springs up to steaming ground and their locations are controlled by a combination of the topography, the geology and the convective plume.

At the base of the model, fluid near the center of the upflow is well within the supercritical regime as temperatures reach 450° C with pressures over 630 bar. Nearer the surface, Figure 3b shows the two-phase nature of the system with a moderately sized natural steam zone forming beneath the clay cap at elevations ranging from 0-600 mRL. The figure also shows the water table level above the reservoir, though the shallow vertical grid resolution does not allow its location to be resolved in detail.

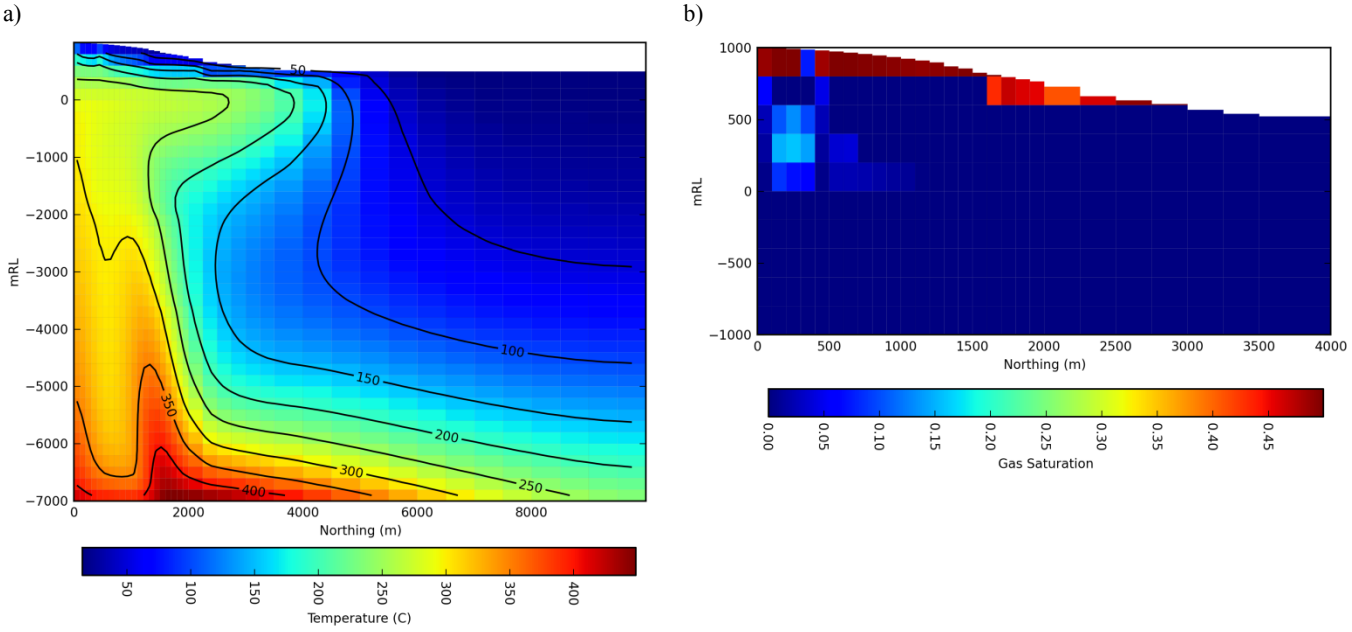

Figure 3: Temperature (a) and gas saturation (b) along line x = 0 m. Note that the plots have different vertical and horizontal scales.

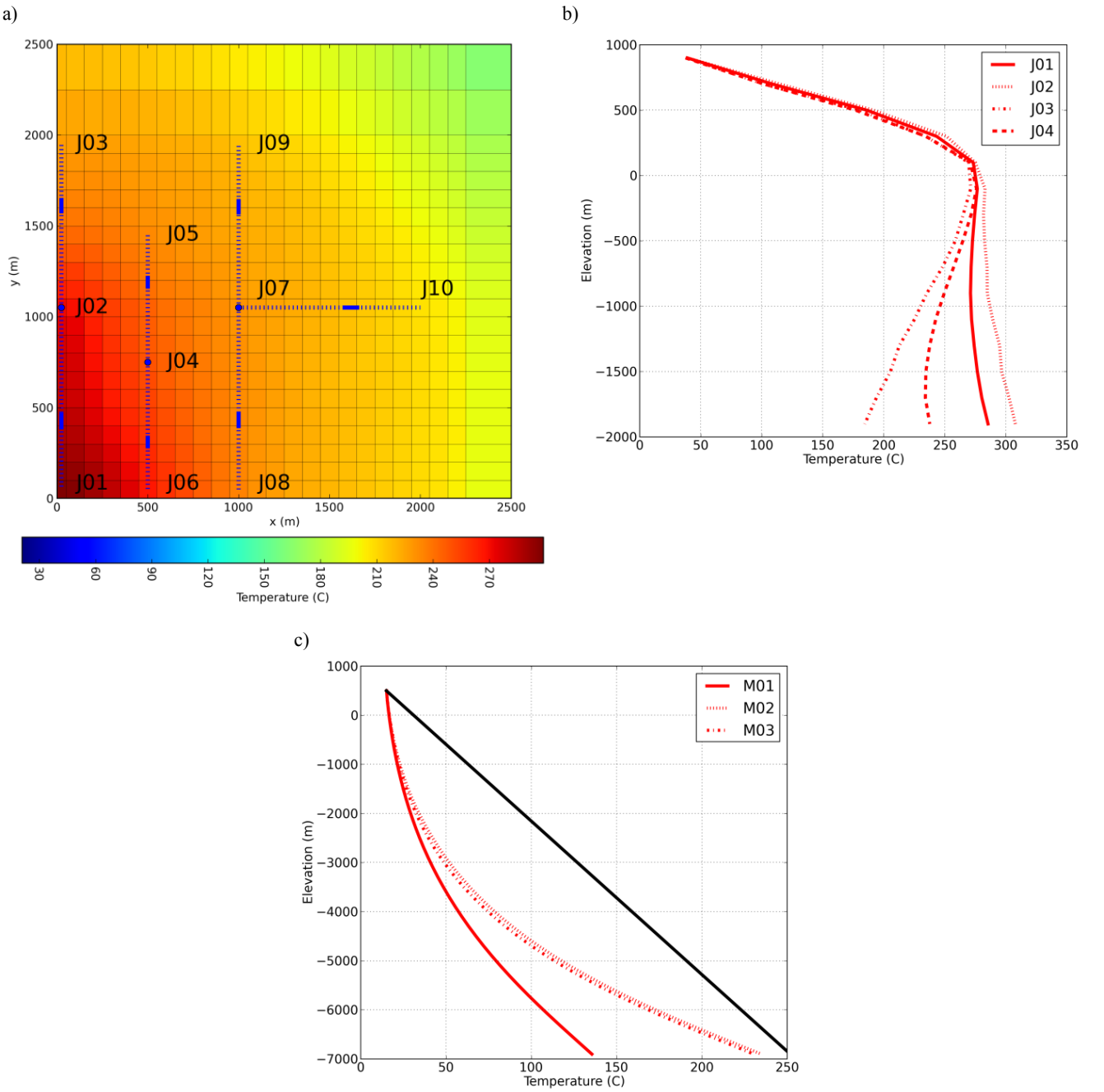

Figure 4: Well locations shown with reservoir temperature at -1000 mRL (a). Solid lines indicate the sections of the well tracks between -1000 and -1200 mRL. Natural state downhole temperatures for selected wells (b). Natural state downhole temperatures for the far-field monitor wells (not shown in (a)). Temperature profile derived from the background heat flux and typical rock conductivity also shown in black (c).

Figure 4a shows the locations and well tracks for 10 wells that were used for simulating a production history for the system. The natural state temperature profiles for a selection of the wells are presented and Figure 4b which shows that they have many familiar characteristics of real geothermal wells. Wells J01 and J02 are located in the middle of the upflow zone and have classic convective profiles. The deviated well J03 and vertical well J04 are closer to the edge of the plume and show typical effects of deeper cold inflows. The far-field temperature profiles obtained from the corner blocks of the model are plotted in Figure 4c and compared with an equivalent conductive profile. They show that the downflow is significant and cool temperatures reach relatively deep elevations as predicted by classical theory (Bredehoeft and Papaopulos, 1965).

In general the results show that the hypothetical model produces synthetic natural state field data with many of the characteristics observed in real hot, liquid-dominated two-phase geothermal systems. The plume is by definition symmetric which makes it difficult to produce some more complicated features such as shallow temperature inversions but nevertheless it provides a rich data set for quantitatively assessing the effects of using different types of bottom boundary conditions when modeling the upper part of the system.

3. THE WORKING MODELS

The objective of this work was to quantitatively assess the accuracy of predictions obtained from models that include only part of the convective plume in their domain, using two different approaches for representing the heat flow from the bottom boundary. To achieve this two working models were created with different bottom boundary conditions. The first model applies uniform background heat flux equal to background heat flux applied at the base of the "true" system. This model will be referred to as the background heat (BH) working model. The second model uses fixed temperature inactive blocks at the bottom boundary and the approach is commonly referred to as a "hot-plate" (Burnell and Kissling, 2005; Bjornsson and Arnaldsson, 2015; Gunnarsson and Aradóttir, 2015; Hernandez *et al*., 2015) leading to the abbreviation (HP) hereafter. Figure 5 shows the vertical extent of the domain of the working models compared to the "true" system model. They both extend down to -3000 mRL giving them a total depth of between 3500 and 4000 m. This puts the bottom boundary more than 1000 m below any potential feedzones and also well into the lower permeability basement formation which is consistent with standard reservoir modeling practice (O'Sullivan *et al*., 2001). It also ensures no supercritical conditions will be encountered in the working models' simulations.

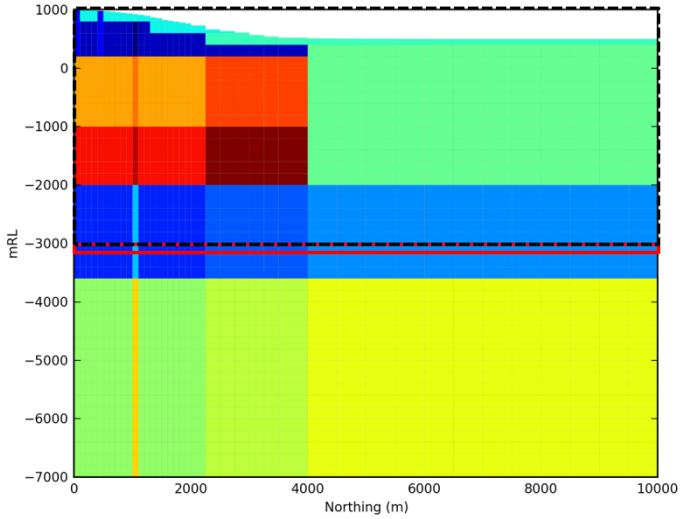

Figure 5: Vertical extents of working models BH and HP (black dotted line) shown with system geology along line x = 0 m. Red solid line indicates the inactive constant temperature layer included in HP.

To isolate the effects of the bottom boundary conditions, all other aspects of the working models were made identical to the "true" system model. The geological structure and formation properties of the "true" system were transferred directly to working models along with the top boundary conditions. The grid structure above -3000 mRL is also identical in the working models and the "true" system model.

In both working models the mass flow applied at the bottom boundary is in accordance with standard practice (O'Sullivan *et al*., 2001). The bottom boundary is closed to mass flow with mass injected into the bottom blocks to represent the deep upflow. The closed boundary prevents any downflow out of the working models which is not consistent with the "true" system but is preferable to open bottom boundary conditions which can have significant, non-physical effects on model results (O'Sullivan *et al*., 2001; Dipippo, 2016). The mass flow magnitudes, their locations and their corresponding enthalpies are calculated directly from the "true" system model. The distribution applied to the bottom of both working models is show in Figure 6a with the negative values being neglected. The total mass injected was 31 kg/s with enthalpies ranging from 650-1430 kJ/kg. Thus the total deep upflow injected into the working models is consistent with the 23 MW measured from "true" system and follows standard modelling practice (O'Sullivan *et al*., 2001).

Figure 6b presents the temperature distribution at -3000 mRL in the "true" system model. This was used to populate the temperatures in the inactive boundary blocks in the HP working model. However, a minimum temperature was enforced throughout the boundary equal to the conductive heat profile corresponding to a heat flux of 80 mW/m^2. This is consistent with the modelling approach when using a "hot-plate" which requires estimating the temperature distribution for the entire bottom boundary (Bjornsson and Arnaldsson, 2015).

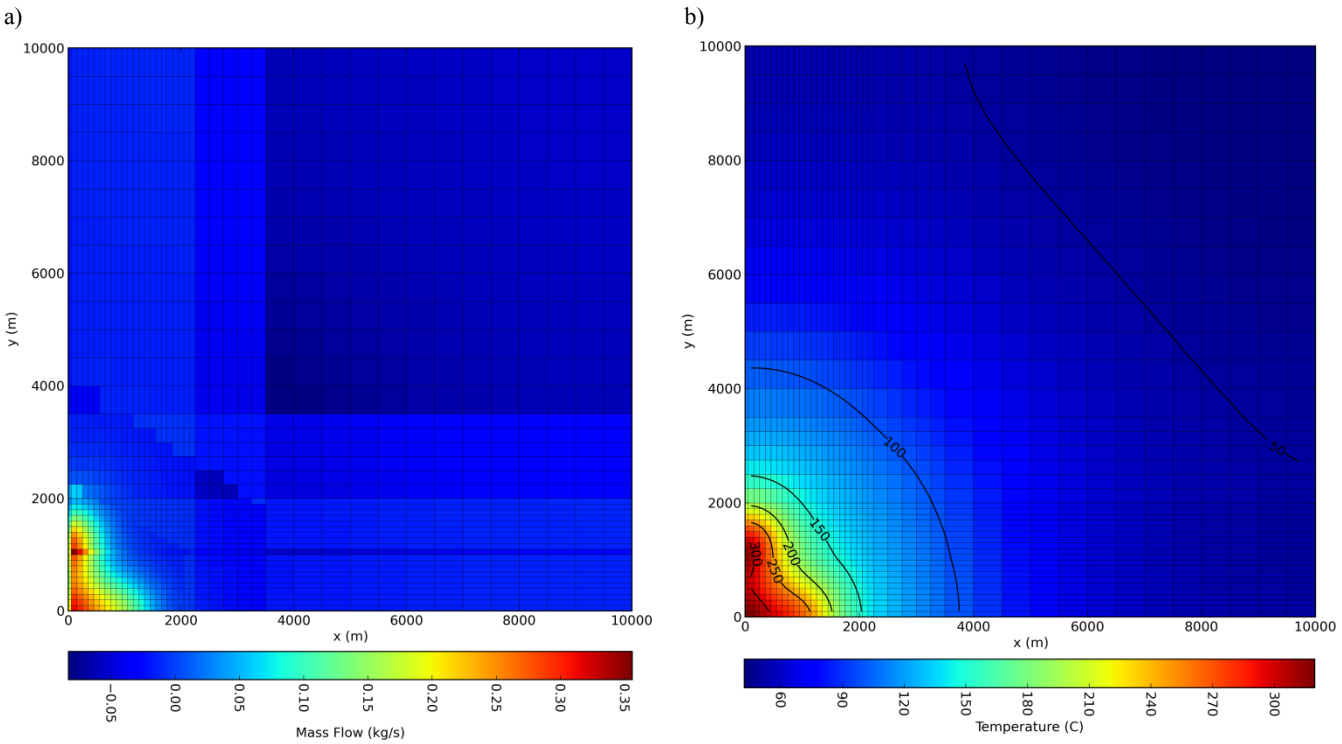

Figure 6: Vertical mass flow (a) and temperature distribution (b) at -3000 mRL from the synthetic model. Positive values for mass flow (a) were used as the deep upflow boundary condition for both working models. The constant temperature boundary condition applied in working model HP uses the results in plot (b).

3.1 Natural State Results

The downhole temperatures predicted by the working models for a selection of wells are presented in Figure 7. At first glance the agreement is excellent in both cases which is to be expected given the level of consistency between the working models and the "true" system model. However, a closer inspection reveals small discrepancies exist with both models predicting slightly lower temperatures than the "true" data between elevations of 0 mRL to -2000 mRL. In both cases this is caused by the closed bottom boundary which forces the convective plume's recharge to take place in a smaller volume, leading to slightly higher lateral cold inflows. Similarly the smaller volume and slightly increased rate of convection pushes the temperature plume in both working models fractionally higher in the shallow zone than the "true" data indicates.

For all four example wells the overestimation of the cold inflow is slightly worse in the HP model than the BH model. There are two main reasons for this result. First, the positive background heat flow imposed at the bottom boundary of the BH model equates to imposing a negative temperature gradient. Plots (c) and (d) in Figure 7 show that a negative temperature gradient at the base of the model helps to restricts the amount of cold inflow at higher elevations, thus improving the match to the "true" data. In contrast, model HP only specifies the temperatures at the bottom boundary and hence does not restrict the cold inflow as much. In spite of this the plots show that beneath the well bores with deeper cold inflow the HP model achieves a better match to "true" data than the BH model because the "true" data has a positive temperature gradient in these zones. The second reason is that for this study the constant temperature boundary condition results in slightly less total conductive heat flow into the bottom of the model at 7.7 MW than the background heat approach which supplies a total of 8 MW.

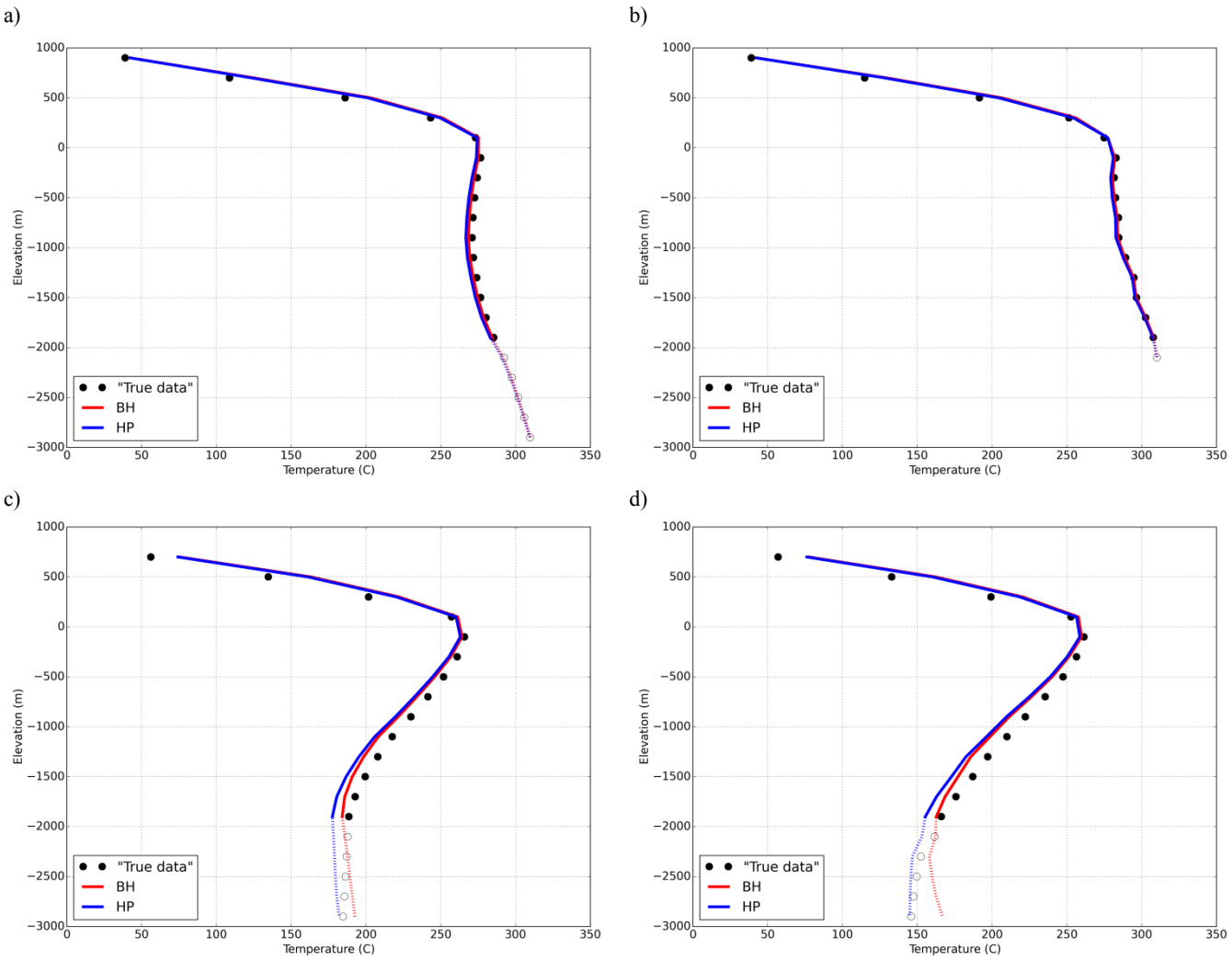

Figure 7: Natural state downhole temperatures for well J01 (a), J02 (b), J07 (c) and J09 (d). Results for working models BH and BH compared with "true data" from the synthetic model. Temperatures from all models also shown for elevations beneath the well bottom.

4. PRODUCTION HISTORY MATCHING

A synthetic production history was generated using the "true" system model to investigate the effects of the bottom boundary conditions on production modeling forecasts. The set of wells used for determining downhole temperatures was also used for the production scenario with the schedule set to achieve production rate equivalent to 120 MW for the entire system. A conversion factor of approximately 2 kg/s of steam per MWe was used based on a hypothetical power plant with a similar configuration to Wairakei (Grant, 2013). This conversion factor results in a target total steam flow of 60 kg/s for the model and the final well schedule which met this criterion is presented in Table 2. The feedzones were selected based on where the well tracks intersected higher permeability faults and also to achieve a good distribution throughout the hot reservoir. Typical productivity indices were assigned to the feedzones which and also given in Table 2.

The same production scenarios were then set up for both working models and the simulations were run using their respective natural states as the initial conditions. Plots comparing the results for the production history forecasts are presented in Figures 8 and 9. Figure 8a shows that both model BH and HP underpredict the total steam flow with the discrepancy increasing over time. After 35 years model BH underpredicts the steam flow by approximately 10% and model HP by approximately 13%. Part of this mismatch is due to differences in average enthalpies predicted by both working models. Figure 8a shows that while their predictions are very close to the "true" data, the small underpredictions increase over time affecting the HP model slightly more than the BH model.

The remaining mismatch in the steam flow is due to increased pressure decline in the feedzones of the working models. This can be observed in the plots of selected feedzone pressures presented in Figure 9. Close inspection reveals that the pressure decline in the deep feedzones is almost identical in both working models but in the shallower feedzones model HP experiences a higher pressure decline than model BH. The causes for this difference are discussed in detail below.

Table 2: Production well feedzone elevations, productivity indices and schedule

Well name	Feedzones	Productivity Indices	Start Year
J01	-240 mRL, -990 mRL	5×10^{-13}	0
J02	-490 mRL, -1490 mRL	5×10^{-13}	0
J04	100 mRL, -1510 mRL	1×10^{-12}	1
J03	190 mRL, -1040 mRL	5×10^{-13}	2
J05	-540 mRL, -1380 mRL	1×10^{-12}	4
J07	-640 mRL, -1240 mRL	1×10^{-12}	10
J06	-300 mRL, -1940 mRL	1×10^{-12}	18
J08	-480 mRL	1×10^{-12}	28
J09	140 mRL, -920 mRL	1×10^{-12}	30
J10	160 mRL, -740 mRL	1×10^{-12}	33

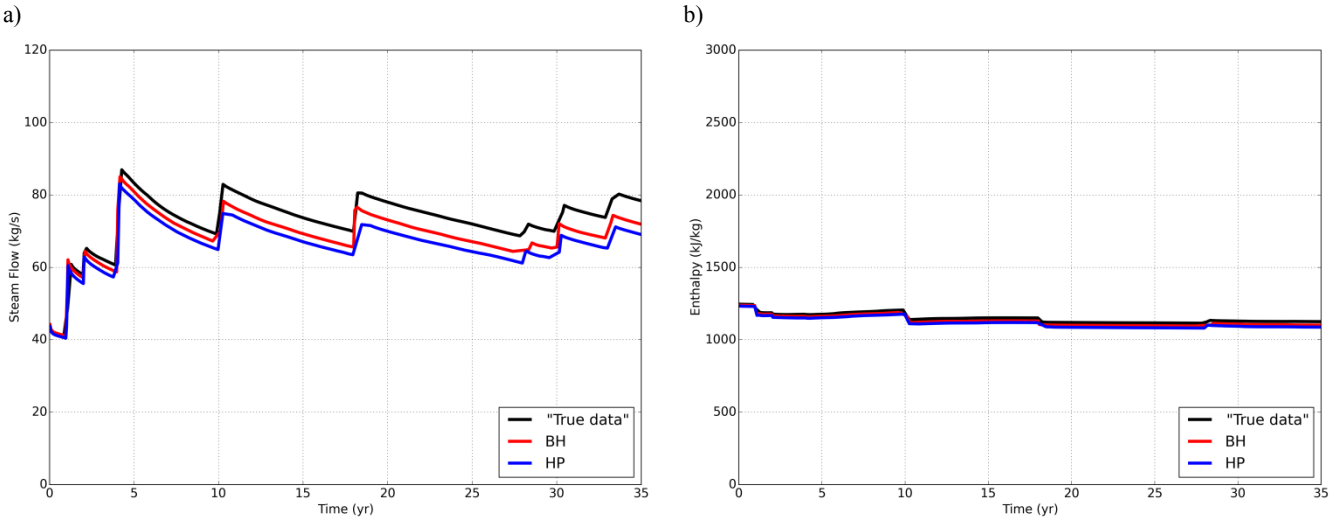

Figure 8: Total steam production (a) and average enthalpy (b) predicted by working models BH and HP compared with "true data" from the synthetic model.

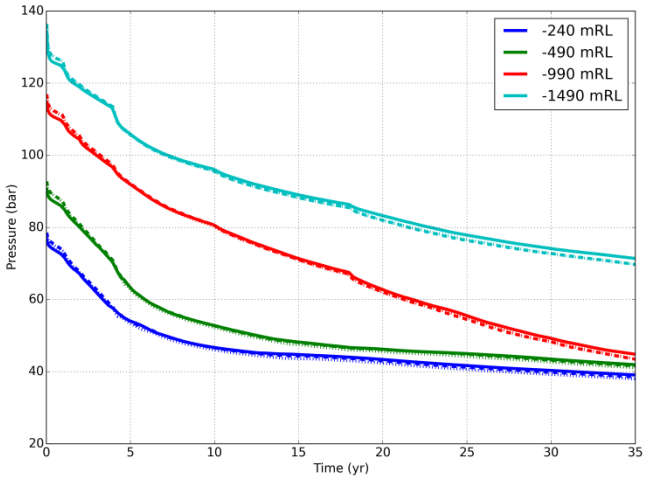

Figure 9: Reservoir pressures taken from the feedzones of J01 and J02 predicted by working models BH (dashes) and HP (dots) compared with "true data" from the synthetic model (solid lines).

To demonstrate these discrepancies more clearly plots of the errors in the predictions made by the working models are presented for well J01 in Figure 10. The errors in the feedzone pressures that increase over time can be explained by the fixed mass flow boundary conditions applied at the bottom of both working models. In the "true" model the deep upflow increases slowly as production decreases the pressure in the reservoir above. This phenomenon is well known and to account for it some reservoir models include time varying mass flows at the bottom boundary (Yeh *et al*., 2014). Figure 10a shows that model HP produces a larger error in the shallow feedzone pressures than model BH despite the same mass flow bottom boundary conditions being applied. This can be explained by considering the downhole temperatures plotted in Figure 7a. The plots show that model HP underpredicts the temperatures in the shallow feedzone by slightly more than the BH model. The lower feedzone temperature results in a correspondingly lower flowing enthalpy as seen in Figure 10c. It also causes lower pressures in the feedzone once boiling begins after approximately 4 years of production and the pressures and temperatures are no longer independent. The extent of the large two-phase region that forms during production is shown in Figure 11 and is consistent with the 30-40 bar total pressure decline experienced.

The increased errors in model HP's predictions for both flowing enthalpy and the shallow feedzone pressure have a cumulative effect leading a larger overall error in its steam flow predictions for individual wells which in turn account for the larger discrepancy in total steam flow.

5. CONCLUSION

A very large supercritical model of an entire hypothetical geothermal system has been developed and it has been used to generate a detailed set of synthetic field data. The effects of two different types of common heat flow bottom boundary conditions were then quantitatively investigated by developing two smaller working models and comparing their natural state and production history predictions with the synthetic field data. The models were developed following standard reservoir modeling practices and only encompassed part of the geothermal plume. The results show that both types of boundary conditions lead to small underpredictions in the natural state downhole temperatures. These errors lead to underpredictions in average enthalpy and total steam flow during production runs. The fixed mass flow applied at the bottom boundary of both models during production simulations contributes to overpredicted pressure declines which also reduce steam flow predictions. For the hypothetical geothermal system investigated in this work the "hot-plate" boundary condition produces slightly larger errors than the background heat approach though this may not necessarily be the case in general.

It is important to note that a small amount of calibration of both models could have corrected the downhole temperatures and enabled them the produce equally good matches to the "true" production data. The calibration process would effectively change the model parameters away from their "true" values as a proxy method of accounting for the systematic model defect created by not including the entire geothermal plume in the model domains (White *et al*., 2014). When calibrating reservoir models of real systems the "true" parameters are never know exactly and this effect always occurs.

Ultimately either approach for modelling the heat flow at the bottom boundary can be used to produce a reservoir model capable of producing accurate predictions of a geothermal system's behaviour. However, the choice of approach affects the calibration process, including the number of parameters that must be calibrated, and either approach may be better suited for calibrating a particular model. Research is in progress to quantify the identifiability of deep permeabilties and other parameters as a result of the approach selected.

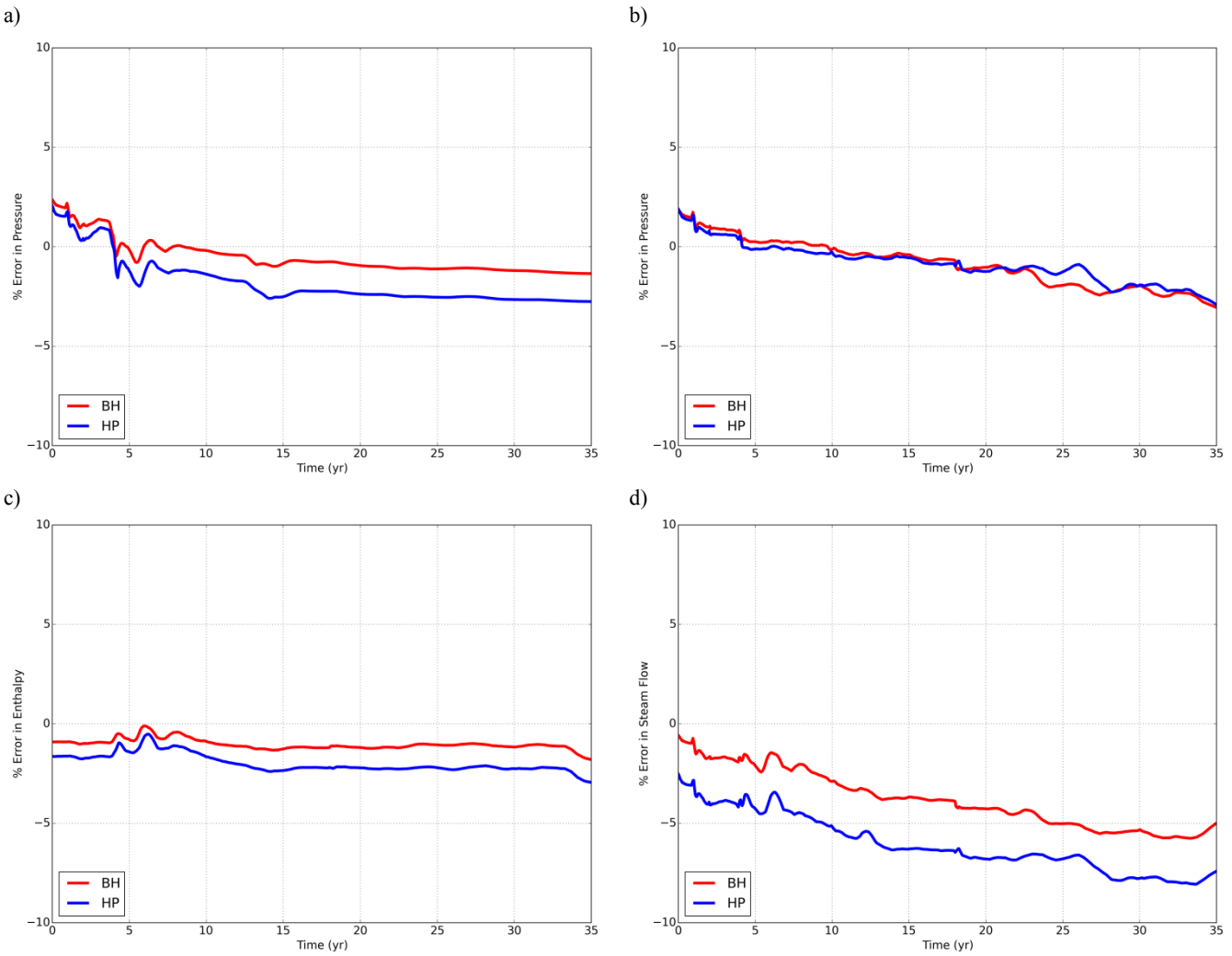

Figure 10: Errors in predictions by the working models for well J01. The plots show the error in the shallow feedzone pressure (a), the deep feedzone pressure (b), flowing enthalpy (c) and steam flow (d).

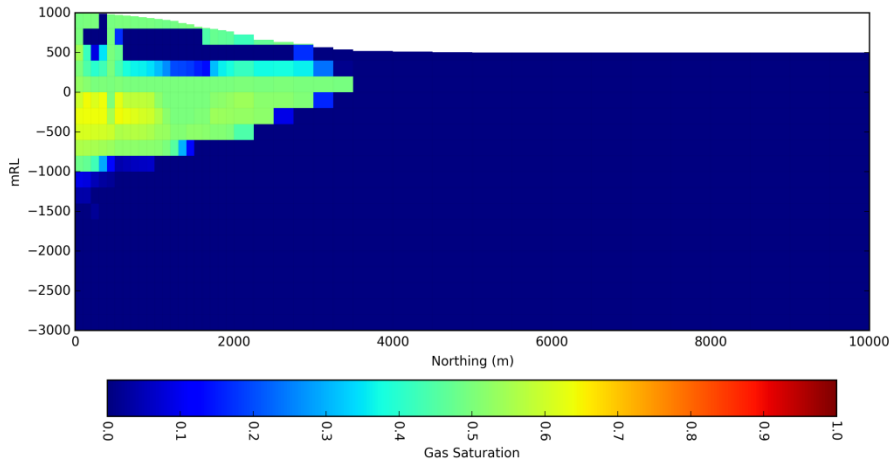

Figure 11: Cross-section from the synthetic model of gas saturation along x = 0 m after 35 years of production.

ACKNOWLEDGEMENTS

The authors acknowledge the support of the NZ Ministry of Business, Innovation and Employment for partially funding this work through the grant: C05X1306, "Geothermal Supermodels". Many thanks also go to Adrian Croucher and David Dempsey for useful discussions and proof-reading.

REFERENCES

Bjornsson, G. and Arnaldsson, A.: Managing large geothermal reservoir models under the iTOUGH2 platform, *Proceedings*, *TOUGH Symposium 2015*, Lawrence Berkeley National Laboratory, Berkeley, California, (2015).

Bredehoeft, J.D. and Papaopulos, I.S.: Rates of vertical groundwater movement estimated from the earth's thermal profile, *Water Resources Research*, **1(2)**, (1965), 325-328.

Burnell J., and Kissling, W.: Rotorua geothermal reservoir modelling part 1: Model update 2004, Industrial Research Limited Report to Environment Bay of Plenty, (2005).

Clearwater, E.K., O'Sullivan, M.J. and Brockbank, K.: An update on modelling the Ohaaki geothermal system, *Proceedings, 33rd New Zealand Geothermal Workshop*, Auckland, New Zealand, (2011).

Croucher, A. E. and O'Sullivan, M. J.: Application of the computer code TOUGH2 to the simulation of supercritical conditions in geothermal systems, *Geothermics*, **37**, (2008), 622-634.

Dipippo, R. (Ed.): *Geothermal Power Generation: Developments and Innovation*, Elsevier Science, (2016).

Grant, M.: *Geothermal Reservoir Engineering*, Elsevier, (2013).

Gunnarsson, G. and Aradóttir, E.S.: The Deep Roots of Geothermal Systems in Volcanic Areas: Boundary Conditions and Heat Sources in Reservoir Modeling, *Transport in Porous Media*, **108 (1)**, (2015), 43-59.

Hernandez, D., Clearwater, J., Burnell, J., Franz, P., Azwar, L. and Marsh, A.: Update on the modeling of the Rotokawa Geothermal System: 2010–2014, *Proceedings*, *World Geothermal Congress*, Melbourne, Australia (2015).

Magnusdottir, L. and Finsterle, S.: An iTOUGH2 equation-of-state module for modeling supercritical conditions in geothermal reservoirs. *Geothermics*, **57**, (2015) 8-17.

O'Sullivan, J., Arthur, S. and O'Sullivan, M.: A new reservoir model to support environmental monitoring of the Orakeikorako geothermal system. *Geothermics*, **59**, (2016), 90-106.

O'Sullivan, J., Kipyego, E., Croucher, A., Ofwona, C. and O'Sullivan, M.: A Supercritical Model of the Menengai Geothermal System, *Proceedings*, *World Geothermal Congress*, Melbourne, Australia (2015).

O'Sullivan, M.J., Pruess, K., and Lippmann, M.J.: State of the art of geothermal reservoir simulation. *Geothermics*, **30 (4)**, (2001), 395-429.

Pruess, K., Oldenburg, K., & Moridis, G.: *TOUGH2 User's Guide, version 2.0*, Lawrence Berkeley National Laboratory, Berkeley, California. (1999).

Ratouis, T.M., O'Sullivan, M.J. and O'Sullivan, J.P.: A Numerical model of Rotorua Geothermal Field, *Geothermics*, **60**, (2016), 105-125.

White, J. T., Doherty, J. E., and Hughes, J. D.: Quantifying the predictive consequences of model error with linear subspace analysis, *Water Resources Research*, **90**, (2014), 1152–1173.

Wellmann, J.F., Croucher, A.E., and Regenauer-Lieb, K.: Python scripting libraries for subsurface fluid and heat flow simulations with TOUGH2 and SHEMAT. *Computers & Geosciences*, **43**, (2012), 197-206.

Yeh, A., O'Sullivan, M.J, Newson, J.A., and Mannington, W.I.: An update on numerical modelling of the Wairakei-Tauhara geothermal system, *Proceedings, 36th New Zealand Geothermal Workshop*, Auckland, New Zealand, (2014).